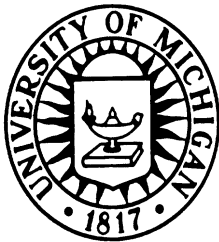# THE UNIVERSITY OF MICHIGAN

COLLEGE OF ENGINEERING
DEPARTMENT OF ELECTRICAL AND COMPUTER ENGINEERING
Radiation Laboratory

SCATTERING AND ABSORPTION OF ELECTROMAGNETIC
RADIATION BY CLOUDS OF DISC SHAPED AEROSOLS

16234-1-F = RL-2290

Final Report on

Grant No. 04-78-B01-1

By

Herschel Weil and C. M. Chu

December 1978

for

National Oceanic and Atmospheric Administration
U.S. Department of Commerce
Boulder, CO 80302

Ann Arbor, Michigan

Scattering and Absorption of Electromagnetic
Radiation by Clouds of Disc Shaped Aerosols

H. Weil and C. M. Chu

1. Introduction

The purpose of this research has been to develop theoretical and numerical procedures which can contribute to the interpretation and prediction of lidar experimental observations of the scattering and absorption of polarized light by snow and ice crystals in cloud formations. Our results can also be used for the study of absorption and scattering of natural unpolarized or partially polarized radiation by any disc-like particles of lossy dielectric material. They can serve as inputs to studies of the influence on cloud formation of radiation absorption, of weather and climate as it is influenced by the greenhouse effect, and of various effects of air pollution.

The scattering and absorption of electromagnetic radiation has been treated purely analytically only for spheres and infinite circular cylinders. For these cases the well known Mie theory is used. For all other cases recourse must be made to numerical (or experimental) methods or to approximate theories such as Rayleigh-Gans or geometric optics which are valid only in the extremes of very long or very short wavelength respectively relative to the body dimensions.

This report describes a numerical technique we have developed to efficiently compute the scattering and absorption by thin circular discs of lossy dielectric (complex refractive index material). Sample numerical results are given for the case of infrared radiation incident on a disc of ice, the wavelengths being comparable to and somewhat less than the disc radius and about 10 times the disc thickness. Such a disc could be thought of as simulating a thin flat plate hexagonal ice crystal, particularly when the crystal is symmetrically rimed. Such crystals fall flat side horizontal in natural clouds (Zikmunda and Vali (1972)) and since their orientation in the horizontal plane is random a circle represents an ensemble average shape as well as approximating the individual crystal.

The work we have done on this grant extends earlier work described in Chu and Weil (1976) and Weil and Chu (1976). In those papers a method,

tailored for its efficient applicability to thin discs, was developed to compute the current density distribution induced by an incident electromagnetic wave of arbitrary polarization and from this to compute the scattered fields and absorbed power. While the method could in principle apply for any directions of incidence relative to the discs, the formulas were in fact worked out and programmed only for incident propagation directions perpendicular or parallel to the flat surfaces of the discs. This of course severely limited the practical situations where the results could be applied. On the present grant, the method was pursued to generate the detailed formulas and associated computing programs for arbitrary directions of incidence. The new program, of course, automatically handles the broadside and edge-on cases when these are called for. It does this in an improved fashion based on some reformulation of the equations used previously.

The present program, incorporating as it does all angles of incidence can now be used with appropriate number densities and probability distributions for crystal dimensions to model the effects of clouds of disc scatterers. However, the only experimental data on size distributions for naturally occurring plate crystals is that summarized in Auer and Veal (1970) which leads to the empirical relation between thickness δ and radius a: $\delta = 2.02 \ (2a)^{0.449} \ \mu m$.

Multiple scattering and absorption (multiple photon-particle interactions) may be treated by radiation transfer computations. Some radiation transfer codes depend intrinsically on the use of Mie theory and so are limited to exploring the effects of spherical particles. The program we have developed for disc particles can however be used as an external subprogram or function input to those radiation codes which are not intrinsically limited to use of Mie theory.

2. The Integral Equation and Reduction to Algebraic Equations

The integral equation for current density J induced in a homogeneous dielectric object of refractive index n is

$$\underset{\sim}{E}^i = \frac{-1}{j\omega\epsilon_0} [\underset{\approx}{L} \cdot \underset{\sim}{J} - \frac{\underset{\sim}{J}}{n^2 - 1}] \tag{1}$$

where $\underset{\approx}{L}$ is the self-adjoint integral operator defined by

$$\underset{\approx}{L} \cdot \underset{\sim}{J} = \iiint_D dv' \underset{\sim}{J}(\underset{\sim}{R}')G(\underset{\sim}{R},\underset{\sim}{R}')$$

$$-\iint_S ds' \underset{\sim}{J}(\underset{\sim}{R}') \cdot \hat{n}'(\underset{\sim}{R}') \nabla G(\underset{\sim}{R},\underset{\sim}{R}'), \tag{2}$$

D and S represent the volume and surface of the object and

$$G = \exp(j|\underset{\sim}{R} - \underset{\sim}{R}'|)/(4\pi|\underset{\sim}{R} - \underset{\sim}{R}'|) . \tag{3}$$

All lengths are normalized by multiplication by $k_0 = 2\pi/\lambda_0$ where λ_0 is the free space wavelength. The time dependence of the fields is assumed to be of the form $e^{j\omega t}$ so that the refractive index n has a negative imaginary part except for ideal nondissipative, nonconductive dielectrics.

Eq. (1) is reduced to a set of linear algebraic equations via the method of moments. To do so $\underset{\sim}{J}(\underset{\sim}{R})$ is expanded in a series of basis functions $\underset{\sim}{W}_j(\underset{\sim}{R})$.

$$\underset{\sim}{J}(\underset{\sim}{R}) = -j\omega\epsilon_0 \sum_j \alpha_j \underset{\sim}{W}_j(\underset{\sim}{R}) . \tag{4}$$

The basis functions should satisfy the requirement

$$\nabla \cdot \underset{\sim}{W}_i = 0 \quad \text{in D}$$

$$\underset{\sim}{W} \cdot \hat{n} \neq 0 \quad \text{on S} \tag{5}$$

to ensure the similar properties (which exist in a homogeneous medium) for $\underset{\sim}{J}(\underset{\sim}{R})$ itself. Substitution of (4) into (1) yields

$$\underset{\sim}{E}^i = \sum_i \alpha_i [\underset{\approx}{L} \cdot \underset{\sim}{W}_i - (1/(n^2 - 1))\underset{\sim}{W}_i] . \tag{6}$$

Using the inner product

$$\langle \underset{\sim}{f}, \underset{\sim}{g} \rangle = \iiint dv' \; \underset{\sim}{f}(\underset{\sim}{R}') \cdot \underset{\sim}{g}(\underset{\sim}{R}') \tag{7}$$

with (4) then yields an algebraic matrix equation to solve for the α_i

$$\langle \underset{\sim}{W}_j, \underset{\sim}{E}^i \rangle = \sum_i \alpha_i [Z_{ij} - W_{ij}/(n^2 - 1)] \tag{8}$$

where

$$Z_{ij} = \langle \underset{\sim}{W}_i, \underset{=}{L} \, \underset{\sim}{W}_j \rangle, \quad W_{ij} = \langle \underset{\sim}{W}_i, \underset{\sim}{W}_j \rangle \; . \tag{9}$$

The symmetric matrix $[Z_{ij} - W_{ij}/(n^2 - 1)]$ is termed an impedance matrix. All material effects are confined to the factor $(n^2 - 1)^{-1}$ while shape effects are included in Z_{ij} and W_{ij}.

To specify the basis functions W_i we use a cylindrical coordinate system (ρ, ϕ, z) with z along the symmetry axis of the disc. The disc fills a region given by $-\delta/2 \le z \le \delta/2, 0 \le \rho \le a$. Then, bearing (5) in mind, we choose the $\underset{\sim}{W}_i$ from the following sets of functions. To most concisely express the induced current when $\underset{\sim}{E}^i$ is perpendicular to $\hat{z}$ we use the TE mode

$$\underset{\sim}{W}_E^{(n,m)} = \nabla \times \{ zR(\rho) Z_n(z) \Phi_m(\phi) \} \tag{10}$$

where

$$Z_n(z) = z^n; \quad \Phi_m(\Phi) = \sin m\phi \quad \text{or} \quad \Phi_m(\phi) = -\cos m\phi. \tag{11}$$

The form of $Z_n(z)$ is chosen to permit easy integration over z when evaluating the impedance expressions. In accord with the thin disc assumption only terms of order δ^2 or greater will be kept in the impedance, hence only $n = 0$ and 1 functions will be needed. The following odd TE modes resulting from the choice of $\sin m\phi$ in (13) result

TEO ODD: $\quad \underset{\sim}{W}_E^{(0,m)} = \hat{\rho}(mR(\rho)/\rho)\sin m\phi + \hat{\phi}R'(\rho)\cos m\phi$

TEl ODD: $\quad \underset{\sim}{W}_E^{(1,m)} = \hat{\rho}(mR(\rho)/\rho)z \sin m\phi + \hat{\phi}R'(\rho)z \cos m\phi \; , \tag{12}$

etc.

Similarly, TM modes defined by

$$\underset{\sim M}{W}^{(n,m)} = \nabla \times \underset{\sim E}{W}^{(n,m)} \tag{13}$$

most concisely express the currents induced when the incident magnetic

field $\underset{\sim i}{H} \perp \hat{z}$. The odd TM nodes are

TM0 ODD: $\underset{\sim M}{W}^{(0,m)} = \hat{z}[(R'(\rho)/\rho) + R''(\rho) - (m^2 R(\rho)/\rho^2)] \sin m\phi$

TM1 ODD: $\underset{\sim M}{W}^{(1,m)} = \hat{\rho}R'(\rho)\sin m\phi + \hat{\phi}(mR(\rho)/\rho)\cos m\phi$

$$+ \hat{z}[-(R'(\rho)/\rho) - R'(\rho) + (m^2 R(\rho)/\rho^2)]\sin m\phi . \tag{14}$$

etc.

For even modes $m\phi$ is to be replaced by $m\phi + (\pi/2)$ in (11) and (14). When neither $\underset{\sim}{E}^i$ nor $\underset{\sim}{H}^i$ are perpendicular to $\hat{z}$, a combination of TE and TM mode $\underset{\sim}{W}$ functions will be required.

With these $\underset{\sim}{W}$ functions there is no coupling between the different values of m; that is, the impedance terms corresponding to use of $\underset{\sim}{W}^{(n,m)}$ and $\underset{\sim}{W}^{(n,m')}$ are zero when $m \neq m'$. Likewise there is no coupling between even and odd modes. We achieve further decoupling by using our assumption that the discs are thin and dropping all terms of order δ^3 or higher relative to the lower order terms when carrying out the volume integrations called for in determining the matrix elements. As a result the impedance matrix has many zero elements and can be partitioned as shown in Eqs. 3.3 - 3.6 of section 3 which greatly facilitates the numerical solution.

In our earlier work involving solely broadside and edge-on incidence only TEO modes were excited and hence only matrix terms involving these modes were not zero [the z(TEO,TEO) terms of the present section 3].

We choose a set of radial functions $R(\rho)$: $\{R_i(\rho)\}$ so as to facilitate the integration. Each $R_i(\rho)$ is chosen to be zero over all but a fractional part of the interval $0 \leq \rho \leq a$. The subintervals are taken small enough to permit the integrals to be evaluated by approximate means with adequate accuracy, yet an excessively large number of intervals is avoided with the choice of $R_i(\rho)$ given below. We are then able

to treat the singularity region to desired accuracy by reducing the problem to the singularity integration for a statics problem plus correction terms, all of which are evaluated analytically. We do end up, however, with rather lengthy expressions for the matrix elements. One needs second derivatives of $R(\rho)$ so we choose symmetric functions made of segments of second order polynomials. Specifically, we divide the interval $0 \leq \rho \leq a$ into N contiguous segments of length a/N. Then the functions $R_i(\rho)$ are the spline functions illustrated schematically in Fig. 1 and defined for $i = 1,2,\ldots,N$ by (15).

$$
\begin{aligned}
&(a/N)(i-1)<\rho<(a/N)i, &&(1/2)(N/a)^2[\rho-(a/N)(i-1)]^2\\[6pt]
&(a/N)i\leq\rho\leq(a/N)(i+1), &&-1+2(N/a)[\rho-(a/N)(i-1)]\\[6pt]
& &&-(1/2)(N/a)^2[\rho-(i-1)(a/N)]^2 \qquad (15)\\[6pt]
&(a/N)(i+1)\leq\rho<(a/N)(i+2) &&-1+2(a/N)[(a/N)(i+3)-\rho]\\[6pt]
& &&-(1/2)(N/a)^2[(a/N)(i+3)-\rho]^2\\[6pt]
&(a/N)(i+2)\leq\rho\leq(a/N)(i+3), &&(1/2)(N/a)^2[(a/N)(i+3)-\rho]^2
\end{aligned}
$$

provided $\rho<a$. For $\rho>a$, $R_i(\rho)=0$. This treatment of the radially dependent part of the problem is typical of techniques used in finite element methods so our numerical method may be thought of as a hybrid moment-finite element method. Note that there is an overlapping of the R_i's in the integrations for Z_{ij} and W_{ij}.
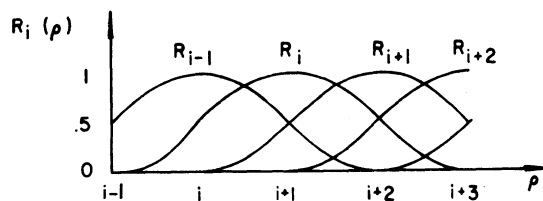
radial distance in units of $\dfrac{a}{N}$

Fig. 1. Illustration of the function defined in Eq. (15).

Numerical evaluation of the integrals is facilitated by use of average values over short intervals for $R_i(\rho)$, and functions involving $R_i(\rho)$, and its derivatives. For this purpose each interval $(a/N)(i-1) < \rho < (a/N)(i+3)$ is subdivided into eight equal parts denoted by $p=1,\ldots,8$ each extending from α_{ip} to β_{ip} and centered on γ_{ip} (see Eqs. 2.5 - 2.7 of section 3). We define averages over these intervals

$$A_{ip} = <R_i(\rho)>_p = (a/2N)^{-1} \int_{\alpha_{ip}}^{\beta_{ip}} R_i(\rho)\,d\rho \qquad (16)$$

and similarly

$$B_{ip} = <R_i'(\rho)>_p, \quad C_{ip} = <R_i(\rho)>_p,$$

$$D_{ip} = <R_i''(\rho)>_p, \quad E_{ip} = <R_i(\rho)/\rho>_p. \qquad (17)$$

Table II in section 3 lists the explicit formulas for $A_{ip} \ldots E_{ip}$.

The W_{ij} and excitation terms $<\underset{\sim}{W}_j \cdot \underset{\sim}{E}^i>$ each involve only a single volume integral and can be evaluated analytically with our choice of polynomial functions for the $R_i(\rho)$ by straightforward integration.

The Z_{ij} each involve double volume and surface integrals with singular integrands. They are carried out by partly numerical and partly analytical methods in which the two z integrations are done analytically to $0(\delta^2)$, the singularities are handled analytically and the two angular integrations reduced to a single integral approximated by a finite sum. The result of the analytic treatment of the singularities plus the use of the averages defined above reduces the radial integrals to finite sums. The results of this somewhat lengthy analysis leads to the formulas which are given in section 3 and where were programmed and used for computation.

Once the α_i and hence $\underset{\sim}{J}$ are determined, classical EM theory permits one to compute the reradiated and the absorbed power by straightforward integrations over the disc volume which can be carried out analytically.

Specifically, the far-zone electric field in the direction $\hat{R}_s(\theta_s,\phi_s)$ may be expressed as

$$\underset{\sim}{E}^s_{Far} = - \frac{j\omega\mu_0 k}{4\pi} \frac{e^{-j\underset{\sim}{R}\cdot\hat{R}_s}}{R} \underset{\sim}{N}(\theta_s,\phi_s) \; e^{j\omega t} \tag{18}$$

where

$$\underset{\sim}{N} = k_0^{-3} \iiint dv' \; e^{-j\underset{\sim}{R}'\cdot\hat{R}_s} \underset{\sim}{J}(R') \; . \tag{19}$$

Then by substituting Eq. 4 for $\underset{\sim}{J}$ one can express $\underset{\sim}{N}$ as

$$\underset{\sim}{N} = -j\omega G_0 k_0^{-2} \sum_k \alpha_k \underset{\sim}{P}_k(\theta_s,\phi_s) \tag{20}$$

where

$$\underset{\sim}{P}_k = I_k^{p^*}(\theta_s,\phi_s)\hat{\theta} + I_k^{s^*}(\theta_s,\phi_s)\hat{\phi} \; . \tag{21}$$

The I_k^p and I_k^s functions are given by Eqs. (4.5) of Section 3 for the present choice of basis functions $\underset{\sim}{W}_k$. They are used also in evaluating the excitations $\underset{\sim}{W}_j, \underset{\sim}{E}^i$ of Eq. (8).

The incident fields are taken to be of unit magnitude with elliptical polarization. They are expressed as

$$\underset{\sim}{E}^i = (p\hat{\theta} + s\hat{\phi})e^{j\omega t} \tag{22}$$

where p and s are complex and satisfy $|p|^2 + |q|^2 = 1$. Then Eqs. (23) - (27) which follow and define the various cross-sections which characterize the scattering and absorption are evaluated. The final formulas which result are given by Eqs. (5.1) - (5.7) of Section 3.

$$\sigma_B(\theta,\phi) = \frac{\text{radiated power per solid angle in direction } (\theta,\phi)}{\text{incident power per area.}} \quad (23)$$

the absorption cross-section

$$\sigma_A = \frac{\text{power dissipated in the object}}{\text{incident power per area}} \quad , \quad (24)$$

the total scattering cross-section,

$$\sigma_{TS} = \int_{4\pi} \sigma_B(\theta,\phi) d\Omega \quad (25)$$

the total cross-section, also called extinction cross section

$$\sigma_T = \sigma_{TS} + \sigma_A \quad (26)$$

and the assymetry factor

$$\sigma_{ASY} = \int \sigma_B(\theta,\phi) \cos\theta_s d\Omega \quad (27)$$

where θ_s is measured relative to the incident direction. σ_B and σ_A are given in terms of the α_i by Eqs. 5.1 and 5.2 of section 3.

3. Computational Formulas

The explicit formulas to be programmed are given in this section.

3.1 Ordering the Coefficients and Partitioning the Matrix

The procedures involve solving the linear algebraic matrix equation (2.8) which we rewrite as

$$\underset{\sim\sim}{z} \, \underset{\sim}{\alpha} = \underset{\sim}{I} \quad (1.1)$$

for unknown vector $\underline{\alpha}$, then computing several functions of the elements α_i of $\underline{\alpha}$. The matrix $\underline{z}$ may be decomposed in the form

$$\underset{\sim\sim}{z} = \underset{\sim\sim}{Z} - \underset{\sim\sim}{W}/(n^2 - 1) \quad (1.2)$$

where the elements of $\underline{Z}$ and $\underline{W}$ depend explicitly on two real parameters a and δ while n^2 is a given complex number. $\underline{I}$, the excitation vector depends on a and δ plus four other real parameters θ_0, ϕ_0, p and s. Each

row of (1.1) (corresponding to the element I_k of $\underline{I}$) is associated with a number of parameters; integers i, j=1...N, m=1...M and "mode labels" TM0, TE0, TM1, even and odd. The association with index k is given by Table I which covers the case m = 1. The k numbering continues from k = 6N+1 through 12N following the same ordering as the m=1 case, but with m=2. This pattern continues until m=M. The maximum k value is K=6NM.

Table I

Index numbers, k, for the excitations
I_k and coefficients α_k

k	mode label	m	i or j	sub-matrix see Eq. (1.4)
1	TM0 ODD	1	1	
⋮	⋮	⋮	⋮	I
N	⋮	⋮	N	
N+1	TE0 ODD	⋮	1	
⋮	⋮	⋮	⋮	
2N	⋮	⋮	N	
2N+1	TM1 ODD	⋮	1	II
⋮	⋮	⋮	⋮	
3N	⋮	⋮	N	
3N+1	TM0 EVEN	⋮	1	
⋮	⋮	⋮	⋮	I
4N	⋮	⋮	N	
4N+1	TE0 EVEN	⋮	1	
⋮	⋮	⋮	⋮	
5N	⋮	⋮	N	
5N+1	TM1 EVEN	⋮	1	II
⋮	⋮	⋮	⋮	
6N	⋮	⋮	N	

Although the overall array of 6NM equations may be large, the solution is reduced analytically to a number of subproblems involving much smaller arrays as follows. First $\underline{z}$ may be shown to reduce to a diagonal array of submatrices so that equation subsets correspondong to "odd" and "even" and to the different m values are uncoupled and may be solved separately. Thus

$$
\underline{\underline{z}} = \begin{bmatrix} \underline{z}(m=1,\ ODD) & 0 & 0 & - - - \\ 0 & \underline{z}(m=1,\ EVEN) & 0 & - - - \\ 0 & 0 & \underline{z}(m=2,\ ODD) & - - - \\ \vdots & \vdots & \vdots & \ddots \end{bmatrix} \tag{1.3}
$$

Furthermore, although the excitations are different for each m in the odd and even cases, the $\underline{z}$'s are not; $\underline{z}(m=m_0,\ ODD) = \underline{z}(m=m_0,\ EVEN) = \underline{z}(m_0)$.

Each of the submatrices $\underline{z}(m)$ may be further partitioned as follows:

$$
\underline{z}(m) = \begin{bmatrix} \underline{z}_I(m) & 0 \\ 0 & \underline{z}_{II}(m) \end{bmatrix} \tag{1.4}
$$

where the $\underline{z}_I(m)$ and $\underline{z}_{II}(m)$ are associated with mode combinations as indicated by the following notation (and by the fifth column of Table I).

$$
\underline{z}_I = \underline{z}(TM0,\ TM0) \tag{1.5}
$$

$$
\underline{z}_{II} = \begin{bmatrix} \underline{z}(TE0,\ TE0) & \underline{z}(TE0,\ TM1) \\ \underline{z}(TM1,\ TE0) & \underline{z}(TM1,\ TM1) \end{bmatrix} \tag{1.6}
$$

In (1.5) and (1.6) the dependance on m is "to be understood". Each of the matrices on the right hand sides is specified by symmetric N x N arrays of complex elements. Thus the largest set of equations which cannot be decoupled has 2N complex unknowns and is a symmetric complex matrix.

3.2 The Matrix Elements Z_{ij}

The individual elements of the submatrices in (1.5) and (1.6) will be expressed in terms of a number of auxiliary functions of the given parameters a and δ. These functions are given in Tables II and III and formulas (2.1) - (2.23). In addition to the subscript index numbers previously introduced (i,j=1...N, m=1...M) there will also be used p,q=1,...N and ℓ=1,...L where N, M and L are all integers whose values must be determined by numerical experimentation but are fixed in a given computer run. To distinguish integer values i and j from the symbol for $\sqrt{-1}$ we use $\hat{j} = \sqrt{-1}$.

The auxiliary functions are

$$R(r,r') = R = (r^2 + r'^2 - 2rr' \cos u + \delta^2)^{1/2} \qquad (2.1)$$

$$R(a,a') = [2a^2(1 - \cos u) + \delta^2]^{1/2} \qquad (2.2)$$

$$D(r,r') = D = R\Big|_{\delta=0} = (r^2 + r'^2 - 2rr' \cos u)^{1/2} \qquad (2.3)$$

$$\delta_i^j = \begin{cases} 0 \text{ if } i \neq j \\ 1 \text{ if } i = j \end{cases} \qquad \text{(The Kronecker } \delta\text{)} \qquad (2.4)$$

$$\alpha_{ip} = (a/N)[i - 1 + (p-1)/2] \qquad (2.5)$$

$$\beta_{ip} = (a/N)(i - 1 + p/2) \qquad (2.6)$$

$$\gamma_{ip} = (a/N)[i - (5/4) + (p/2)] = (1/2)(\alpha_{ip} + \beta_{ip}) \qquad (2.7)$$

$$u_{\ell} = (\pi/L)[\ell - (1/2)] \tag{2.8}$$

$$F(i,p;j,q) = F(\beta_{ip},\beta_{jq}) + F(\alpha_{ip},\alpha_{jq})$$
$$- F(\beta_{ip},\alpha_{jq}) - F(\alpha_{ip},\beta_{jq}) \tag{2.9}$$

$$F(r,r') = r'\ell n(r-r'\cos u + R) + r\,\ell n(r'-r\cos u + R)$$
$$+ 2(\sin u)/\delta\;\{r'^{2}\tan^{-1}[r'\delta\sin u/[(r-r'\cos u)R + D^{2}]]$$
$$+ r^{2}\tan^{-1}[r\delta\;\sin u/[(r'-r\cos u)R + D^{2}]]\}$$
$$+ (D^{2}\cos u - 2rr'\sin^{2}u)\{R - D - 2\delta\;\ell n[(\delta+R)/D]\}/\delta^{2}$$
$$-(\sin^{2}u/\delta^{2})\{r'^{3}\ell n[(r-r'\cos u + R)/(r-r'\cos u + D)]$$
$$+ r^{3}\;\ell n[(r'-r\cos u + R)/(r'-r\cos u + D)]\} \tag{2.10}$$

$$G(j,q) = G(\beta_{jq}) - G(\alpha_{jq}) \tag{2.11}$$

$$G(r) = \ell n[r-a\cos u + R(a,r)]$$
$$+ (a/\delta)\sin u\,\tan^{-1}\{a\delta\;\sin u/[D(a,r) + (r-a\cos u)R(a,r)]\}$$
$$+ \ell n\{[\delta + R(a,r)]/D(a,r)\}/\delta \tag{2.12}$$

$$H(i,p;j,q) = H(\beta_{ip},\beta_{jq}) + H(\alpha_{ip},\alpha_{jq})$$
$$- H(\beta_{ip},\alpha_{jq}) - H(\alpha_{ip},\beta_{jq}) \tag{2.13}$$

$$H(r,r') = \{r'\ell n[(r-r'\cos u + D)/(r-r'\cos u + R)]*$$

$$*H(0,0) = -\frac{u}{\delta\sin u}$$

$$+ r\ln[(r-r'\cos u + D)/(r'-r\cos u + R)]$$

$$- (\delta/\sin u)\tan^{-1}[(R\delta\sin u)/(rr'\sin^2 u + \delta^2\cos u)]\}/\delta^2 \tag{2.14}$$

$$K(U) = (2/\delta)\ln[(R(a,a) + \delta)/D(a,a)]$$

$$- (2/\delta^2)[R(a,a) - D(a,a)] - \hat{j} \tag{2.15}$$

$$S(i,p;j,q) = S(\beta_{ip},\beta_{jq}) + S(\alpha_{ip},\alpha_{jq})$$

$$- S(\beta_{ip},\alpha_{jq}) - S(\alpha_{ip},\beta_{jq}) \tag{2.16}$$

$$S(r,r') = r\ln(r'-r\cos u + D)$$

$$+ r'\ln(r-r'\cos u + D) \tag{2.17}$$

Table II

Mean Values of the Radial Functions

q	A_{iq}	B_{iq}	C_{iq}	D_{iq}	E_{iq}
1	$\frac{1}{24}$	$-\frac{1}{6} + \frac{1}{4}i$	$\frac{1}{4}$	$i - \frac{3}{4}$	$\frac{5}{8} - \frac{i}{2} + (i-1)^2\ln\frac{2i-1}{2i+2}$
2	$\frac{7}{24}$	$-\frac{1}{6} + \frac{3}{4}i$	$\frac{3}{4}$	$i - \frac{1}{4}$	$\frac{7}{8} - \frac{i}{2} + (i-1)^2\ln\frac{2i}{2i-1}$
3	$\frac{17}{24}$	$\frac{1}{6} + \frac{3}{4}i$	$\frac{3}{4}$	$-i - \frac{1}{4}$	$\frac{7}{8}+\frac{i}{2} - (i^2+2i-1)\ln\frac{2i+2}{2i+1}$
4	$\frac{23}{24}$	$\frac{1}{6} + \frac{1}{4}i$	$\frac{1}{4}$	$-i - \frac{3}{4}$	$\frac{5}{8}+\frac{i}{2} - (i^2+2i-1)\ln\frac{2i+2}{2i+1}$
5	$\frac{23}{24}$	$-\frac{1}{3} - \frac{1}{4}i$	$-\frac{1}{4}$	$-i - \frac{5}{4}$	$\frac{3}{8}+\frac{i}{2} - (i^2+2i-1)\ln\frac{2i+3}{2i+2}$
6	$\frac{17}{24}$	$-\frac{4}{3} - \frac{3}{4}i$	$-\frac{3}{4}$	$-i - \frac{7}{4}$	$\frac{5}{8}+\frac{i}{2} - (i^2+2i-1)\ln\frac{2i+3}{2i+2}$
7	$\frac{7}{24}$	$-\frac{5}{3} - \frac{3}{4}i$	$-\frac{3}{4}$	$i + \frac{a}{4}$	$-\frac{15}{8} -\frac{i}{2} + (i+3)^2\ln\frac{2i+5}{2i+4}$
8	$\frac{1}{24}$	$-\frac{2}{3} - \frac{1}{4}i$	$-\frac{1}{4}$	$i + \frac{11}{4}$	$-\frac{13}{8} -\frac{i}{2} + (i+3)^2\ln\frac{2i+6}{2i+5}$

The following combinations of the functions in Table II occur frequently here and in Section 4.

$$F_{iq}(m) = F_{iq} = (C_{iq} + D_{iq} - m^2 E_{iq})(N/A) \qquad (2.18)$$

$$G^{jq}_{ip}(m) = G^{jq}_{ip} = m^2 A_{ip} A_{jq} + B_{ip} B_{jq} \qquad (2.19)$$

$$H^{jq}_{ip}(m) = H^{jq}_{ip} = m(A_{ip} B_{jq} + B_{ip} A_{jq}) \qquad (2.20)$$

$$P_{iq}(m) = mA_{iq} + B_{iq}, \quad M_{iq}(m) = mA_{iq} - B_{iq} \qquad (2.21)$$

Table III

Summation Limits p_0 and q_0

i	$p_0, \ q_0$
$\leq N - 3$	8
$N - 2$	6
$N - 1$	4
N	2

Further auxiliary functions are

$$\xi_{ij} = \sum_{p=1}^{P_0} \sum_{q=1}^{q_0} \{e^{-\hat{j}D(\gamma_{ip},\gamma_{jq})}[(1 + jD(\gamma_{ip},\gamma_{jq}))$$

$$F(i,p;j,q) - \hat{j} \, a^2/(2N)^2][G^{iq}_{ip} \cos mu \cos u$$

$$+ H^{jq}_{ip} \sin mu \sin u]\}_{u=u\ell} \qquad (2.22)$$

and

$$\zeta_{ij} = \sum_{p=1}^{P_0} \sum_{q=1}^{q_0} \{e^{-\hat{j}D(\gamma_{ip},\gamma_{jq})}[(1 + jD(\gamma_{ip},\gamma_{jq}))$$

$$F(i,p;j,q) - \hat{j} \, a^2/(2N)^2][G^{jq}_{ip} \sin mu \sin u$$

$$+ H^{jq}_{ip} \cos mu \cos u]\}_{u=u\ell} \qquad (2.23)$$

Note that ξ_{ij} is obtained from ξ_{ij} by interchanging H_{ip}^{jq} and G_{ip}^{jq}.

In terms of all the above auxiliary functions the impedance submatrices are

TM0, TM0

$$Z_{ij}(\text{TM}\,0,\,\text{TM}\,0) = \pi\delta^2/(2L) \sum_{\ell=1}^{L} \cos m\, u_\ell$$

$$[\sum_{p=1}^{P_0} \sum_{q=1}^{q_0} e^{-\hat{j}D(\gamma_{ip},\gamma_{jq})} F_{iq}F_{jq}[(1 + jD(\gamma_{ip},\gamma_{jq}))$$

$$(F(i,p;j,q) - 2H(i,p;j,q)) - \hat{j}\, a^2/(2N)^2]\}_{u=u_\ell} \qquad (2.24)$$

TE0, TE0

$$Z_{ij}(\text{TE}\,0,\,\text{TE}\,0) = \pi\delta^2/(2L) \sum_{\ell=1}^{L} \{\xi_{ij} - e^{-\hat{j}D(a,a)} \cos mu$$

$$m^2 K(u)[(1/2)\delta_N^i + \delta_{N-1}^i + (1/2)\delta_{N-2}^i][(1/2)\delta_N^j + \delta_{N-1}^j +$$

$$(1/2)\delta_{N-2}^j]\}_{u=u_\ell} \qquad (2.25)$$

TE0, TM1

$$Z_{ij}(\text{TE}\,0,\,\text{TM}1) = \pi\delta^2/(2L) \sum_{\ell=1}^{L} \{\zeta_{ij} + m \cos mu$$

$$[(1/2)\delta_N^i + \delta_{N-1}^i + (1/2)\delta_{N-2}^i] \sum_{q=1}^{q_0} \{e^{-\hat{j}D(a,\gamma_{jq})} F_{jq}$$

$$[(1 + \hat{j}D(a, \gamma_{jq}))G(j,q) - \hat{j}\, a/(2N)]\}$$

$$-mNe^{-\hat{j}D(a,a)} \cos mU \cdot K(u)[(1/2)\delta_N^i + \delta_{N-1}^i + (1/2)\delta_{N-2}^i]$$

$$(\delta_N^j - \delta_{N-2}^j)_{u=u_\ell} \qquad (2.26)$$

TM1, TM1

$$Z_{ij}(\text{TM}1,\,\text{TM}1) = \pi\delta^2/(2L) \sum_{\ell=1}^{L} \{\xi_{ij}$$

$$-\cos mu [\sum_{p=1}^{p_0} \sum_{q=1}^{q_0} [e^{-\hat{j}D(\gamma_{ip},\gamma_{jq})} [(1 + \hat{j}D(\gamma_{ip},\gamma_{jq}))$$

$$S_\ell(i,p;j,q) - \hat{j} \, a^2/(2N)^2] \, F_{ip}F_{jq}]$$

$$-N \sum_{p=1}^{p_0} [e^{-\hat{j}D(a,\gamma_{ip})} [(1 + \hat{j}D(a,\gamma_{ip}))G(i,p)$$

$$-\hat{j} \, a/(2N)](\delta_N^j - \delta_{N-2}^j)F_{ip}]$$

$$-N \sum_{q=1}^{q_0} [e^{-\hat{j}D(a,\gamma_{jq})} [1 + \hat{j}D(a,\gamma_{jq}))G(j,q)$$

$$-\hat{j} \, a/(2N)](\delta_N^i - \delta_{N-2}^i) \, F_{jq}]$$

$$+N^2 e^{-\hat{j}D(a,a)}K(U)(\delta_N^i - \delta_{N-2}^i)(\delta_N^j - \delta_{N-2}^j)]\}_{u=u_\ell} \qquad (2.27)$$

3.3 The Matrix Elements W_{ij}

The W_{ij} will be expressed in terms of the integrals $I_{m(n+1)}(a) = \int_0^1 \frac{x^n dx}{(x+a)^m}$ with explicit expressions as follows provided $a \neq 0$. In this section a is not the radius of the disc which is denoted by $\tilde{a}$.

m=1

$$I_{11} = \ln\frac{1+a}{a}$$

$$I_{1n} = \frac{1}{n-1} - a \, I_{1(n-1)}, \quad n=2,3,4,5$$

m=2

$$I_{21} = \frac{1}{a(1+a)}$$

$$I_{22} = -\frac{1}{1+a} + \ln\frac{1+a}{a}$$

$$I_{2n} = \frac{1}{(1+a)(n-2)} - \frac{(n-1)a}{n-2} \, I_{2(n-1)}, \quad n=3,4,5$$

m=3

$$I_{31} = -\frac{1}{2} \left[\frac{1}{(1+a)^2} - \frac{1}{a^2} \right]$$

$$I_{33} = \frac{(4+3a)a}{2(1+a)^2} - \frac{3}{2} + \ln \frac{1+a}{a}$$

$$I_{3n} = \frac{1}{(1+a)^2(n-3)} - \frac{(n-1)a}{n-3} I_{3(n-1)}, \quad n-2,4,5$$

m=4

$$I_{41} = -\frac{1}{3} \left[\frac{1}{(1+a)^3} - \frac{1}{a^3} \right]$$

$$I_{44} = \frac{3a+(a/2)a^2+(11/6)a^3}{(1+a)^3} - \frac{11}{6} + \ln \frac{1+a}{a}$$

$$I_{4n} = \frac{1}{(1+a)^3} \frac{1}{n-4} - \frac{(n-1)a}{n-4} I_{4(n-1)}, \quad n=2,3,5 \qquad (3.4)$$

These integrals will be used to express a number of functions $f_1 \ldots f_4$, $g_1 \ldots g_3$, h_1, h_2 and $W_{i,i+3}$ as shown in Table IV.

Table IV

Structure of W_{ij}

i	$W_{i,i}$	$W_{i,i+1}$	$W_{i,i+2}$	$W_{i,i+3}$
N	f_1	0	0	0
N-1	f_1+f_2	g_1	0	0
N-2	$f_1+f_2+f_3$	g_1+g_2	h_1	0
$\leq$ N-3	$f_1+f_2+f_3+f_4$	$g_1+g_2+g_3$	h_1+h_2	$W_{i,i+3}$

The f_i, g_i and h_i functions are different for each submatrix. In their formulas we have not written the argument a explicitly in each $I_{mn}(a)$. Note that a takes on different values in different formulas. Two

special cases corresponding to a=0 occur. These are for f_1 when i=1 and are treated separately in footnotes.

TMO - TMO

$$f_1 = \pi\delta(N/\tilde{a})^2[(3/2)+a+I_{13}-m^2(I_{13}+I_{24})$$

$$+ (m^4/4)I_{35}]_{a=i-1,i\neq1}*$$

$$f_2 = \pi\delta(N/\tilde{a})^2[a-(1/2)+I_{11}- 2I_{12}+ I_{13}$$

$$+ m^2(I_{11}+ 2I_{12}- I_{13}- I_{21}- I_{22}+ 3I_{23}- I_{24})$$

$$+ (m^4/4)(I_{31}+ 4I_{32}+ 2I_{33}-4I_{34}+ I_{35})]_{a=i}$$

$$f_3 = \pi\delta(N/\tilde{a})^2[(3/2)+ a+ I_{13}$$

$$+ m^2(2I_{11}- I_{13}+ 2I_{22}- I_{24})$$

$$+ (m^4/4)(4I_{31}- 4I_{33}+ I_{35})]_{a=i+1}$$

$$f_4 = \pi\delta(N/\tilde{a})^2[-(1/2)+ a+ I_{11}- 2I_{12}+ I_{13}$$

$$+ m^2(-I_{11}+ 2I_{12}- I_{13}+ I_{21}- 3I_{22}+ 3I_{23}- I_{24})$$

$$+ (m^4/4)(I_{31}- 4I_{32}+ 6I_{33}- 4I_{34}+ I_{35})]_{a=i+2}$$

$$g_1 = \pi\delta(N/\tilde{a})^2[-(1/2)- a+ I_{11}-I_{12}$$

$$-(m^2/2)(I_{11}+ 2I_{12}- 2I_{13}+ I_{22}+ 3I_{23}- 2I_{24})$$

$$+ (m^4/4)(I_{33}+ 2I_{34}- I_{35})]_{a=i}$$

$$g_2 = \pi\delta(N/\tilde{a})^2[(1/2)+ a- I_{12}+ I_{13}$$

---

*When a=i-1,i=1 so that a=0

$$f_1 = (\pi\delta/2)(N/\tilde{a})^2[4-2m^2+(m^4/4)]$$

$$+ (m^2/2)(3I_{11}+ 2I_{12}- 2I_{13}- 2I_{21}+ 3I_{22}+ 3I_{23}- 2I_{24})$$

$$+ (m^4/4)(2I_{31}+ 4I_{32}- 3I_{33}- 2I_{34}+ I_{23})]_{a=i+1}$$

$$g_3 = \pi\delta(N/\tilde{a})^2[-(1/2)- a+ I_{12}- I_{13}$$

$$+ (m^2/2)(-I_{11}- 2I_{12}+ 2I_{13}+ 2I_{21}- I_{22}- 3I_{23}+ 2I_{24})$$

$$+ (m^4/4)(2I_{31}- 4I_{32}+ I_{33}+ 2I_{34}- I_{35})]_{a=i+2}$$

$$h_1 = \pi\delta(N/\tilde{a})^2[-(3/2)- a- I_{13}$$

$$+ m^2(-I_{11}+ I_{23}- I_{22}+ I_{24})$$

$$+ (m^4/4)(2I_{33}- I_{35})]_{a=i+1}$$

$$h_2 = \pi\delta(N/\tilde{a})^2[(1/2)- a- I_{11}+ 2I_{12}- I_{13}$$

$$+ m^2(-2I_{12}+ I_{13}+ 2I_{22}- 3I_{23}+ I_{24})$$

$$+ (m^4/4)(I_{31}- 4I_{33}+ 4I_{34}- I_{35})]_{a=i+2}$$

$$W_{i,i+3} = \pi\delta(N/\tilde{a})^2[-(1/2)+ a- I_{12}+ I_{13}$$

$$-(m^2/2)(I_{11}- 2I_{12}+ 2I_{13}+ I_{22}- 3I_{23}+ 2I_{24})$$

$$+ (m^4/4)(I_{33}- 2I_{34}+ I_{35})]_{a=i+2}$$

TE0 - TE0 and TM1 - TM1

These two cases have identical $W_{i,j}$

$$f_1 = \pi\delta[(1/4)+(a/3)+(m^2/4)I_{15}]_{a=i-1,i\neq1}{}^*$$

---

*When a=i-1, i=1 so that a=0

$$f_1 = (\pi\delta/4)[1 + (m^2/4)]$$

$$f_2 = \pi\delta[(1/12) + (a/3)$$

$$+ (m^2/4)(I_{11} + 4I_{12} + 2I_{13} - RI_{14} + I_{15})]_{a=i}$$

$$f_3 = \pi\delta[(1/4) + (a/3)$$

$$+ (m^2/4)(4I_{11} - 4I_{13} + I_{15})]_{a=i+1}$$

$$f_4 = \pi\delta[(1/12) + (a/3)$$

$$+ (m^2/4)(I_{11} - 4I_{12} + 6I_{13} - 4I_{14} + I_{15})]_{a=i+2}$$

$$g_1 = \pi\delta[(1/12) + (a/6)$$

$$+ (m^2/4)(I_{13} + 2I_{14} - I_{15})]_{a=i}$$

$$g_2 = \pi\delta[-(1/12) - (a/6)$$

$$+ (m^2/4)(2I_{11} + 2I_{12} - 2I_{13} - 2I_{14} + I_{15})]_{a=i+1}$$

$$g_3 = \pi\delta[(1/12) + (a/6)$$

$$+ (m^2/4)(2I_{11} - 4I_{12} + I_{13} + 2I_{14} - I_{15})]_{a=i+2}$$

$$h_1 = \pi\delta[-(1/4) - (a/3)$$

$$+ (m^2/4)(2I_{13} - I_{15})]_{a=i+1}$$

$$h_2 = \pi\delta[-(1/12) - (a/3)$$

$$+ (m^2/4)(I_{11} - 4I_{13} - I_{15})]_{a=i+2}$$

$$W_{i,i+3} = \pi\delta[-(1/12) - (a/6)$$

$$+ (m^2/4)(I_{13} - 2I_{14} + I_{15})]_{a=i+2}$$

TEϕ - TM1

$$f_1 = \pi\delta m/4$$

$$f_2 = \pi\delta m(3/4)$$

$$f_3 = -\pi\delta m(3/4)$$

$$f_4 = -\pi\delta m/4$$

$$g_1 = \pi\delta m/2$$

$$g_2 = 0$$

$$g_3 = -\pi\delta m/2$$

$$h_1 = \pi\delta m/4$$

$$h_2 = -\pi\delta m/4$$

$$w_{i,i+3} = 0$$

In this case (TE0-TM1) the results of applying Table IV may be summarized as in Table V. This can give an easy check on a bit of the programming.

Table V

$W_{i,j}$ for TE0-TM1 Case

W \ i	N	N-1	N-2	≤N-3
$W_{i,i}$	1/4	1	1/4	0
$W_{i,i+1}$	0	1/2	1/2	0
$W_{i,i+2}$	0	0	1/4	0
$W_{i,i+3}$	0	0	0	0

4. The Excitations $I_k(\theta_0, \phi_0)$

The index k is determined by the scheme in Table I. It will facilitate writing the subsequent formulas to introduce the notation

$$m = 6N(m-1) \tag{4.1}$$

In the following $J_n(x)$ indicates the Bessel function of the first kind of order m and argument x. We will use the following auxiliary functions $I_{Ik} - I_{IIIk}$ to define the $I_k(\theta,\phi)$. For excitations we use $\theta=\theta_0$, $\phi=\phi_0$ but the same I_k functions, evaluated for other θ,ϕ values, are needed in Section 5.

$$I_{Ik}(\theta) = \Pi \sum_{p=1}^{P_0} F_{kp}(m) \; J_m(\gamma_{kp} \sin\theta) \qquad (4.2)$$

$$I_{IIk}(\theta) = \Pi \sum_{p=1}^{P_0} \{P_{kp}(m) J_{m-1}(\gamma_{kp} \sin\theta) - M_{kp}(m) J_{m+1}(\gamma_{kp} \sin\theta)\}$$

$$I_{IIIk}(\theta) = \Pi \sum_{p=1}^{P_0} P_{kp}(m) \{J_{m-1}(\gamma_{kp} \sin\theta) + M_{kp}(m) J_{m+1}(\gamma_{kp} \sin\theta)\}$$

Here $F_{kp}(m)$, $P_{kp}(m)$ and $M_{kp}(m)$ are given by (2.18) and (2.21); the constant Π is defined as

$$\Pi = \pi\delta(-\hat{j})^{m-1} a/(2N) \qquad (4.3)$$

Each I_k is decomposed into two parts with factors p and s, $0 \leq |p| \leq 1$, $0 \leq |s| \leq 1$, $|p|^2 + |s|^2 = 1$, and p and s either real or imaginary. Then

$$I_k(\theta,\phi) = pI_k^p(\theta,\phi) + sI_k^s(\theta,\phi) \qquad (4.4)$$

(The symbols p and s stand for the German words parallel and senkrecht meaning parallel and perpendicular.) The I_k^p and I_k^s are specified as follows:

<u>$1 + m \leq k \leq N + m$</u>   (TMO ODD)

$$I_k^p(\theta,\phi) = 2\hat{j}^{-1} \sin\theta \; \sin m\phi \; I_{Ik}(\theta)$$

$$I_k^s(\theta,\phi) = 0$$

$\underline{N + 1 + m \leq k \leq 2N + m}$ (TE0 ODD)

$$I_k^p(\theta,\phi) = \cos\theta \, \sin m\phi \, I_{IIk'}(\theta)$$

k' = k-(n+m)

$$I_k^s(\theta,\phi) = \cos m\phi \, I_{IIIk'}(\theta)$$

$\underline{2N + 1 + m \leq k \leq 3N + m}$ (TM1 ODD)

$$I_k^p(\theta,\phi) = \cos\theta \, \sin m\phi \, I_{IIIk'}(\theta)$$

k' = k-(2N + m)

$$I_k^s(\theta,\phi) = \cos m\phi \, I_{IIk'}(\theta)$$

$\underline{3N + 1 + m \leq k \leq 4N + m}$ (TM0 EVEN)

$$I_k^p(\theta,\phi) = 2\hat{j}^{-1} \sin\theta \, \cos m\phi \, I_{Ik'}(\theta)$$

k' = k-(3N + m)

$$I_k^s(\theta,\phi) = 0$$

(4.5)

$\underline{4N + 1 + m \leq k \leq 5N + m}$ (TE0 EVEN)

$$I_k^p(\theta,\phi) = \cos\theta \, \cos m\phi \, I_{IIk'}(\theta)$$

k' = k-(4N + m)

$$I_k^s(\theta,\phi) = -\sin m\phi \, I_{IIIk'}(\theta)$$

$\underline{5N + 1 + m \leq k \leq 6N + m}$ (TM1 EVEN)

$$I_k^p(\theta,\phi) = \cos\theta \, \cos m\phi \, I_{IIIk'}(\theta)$$

k' = k-(5N + m)

$$I_k^s(\theta,\phi) = -\sin m\phi \, I_{IIk'}(\theta)$$

5. Cross-Sections

Once the α_k are computed for a given set of data $(\theta_0, \phi_0, p, s;$ a, δ, n), one or more of the quantities given below will be desired. The formulas use notation $|A|$, $I_m(A)$ and A* for absolute value, imaginary part and complex conjugate of complex quantity A.

Bistatic or differential cross-section

$$\sigma_B(\theta_s,\phi_s) = (4\pi k_0)^{-2} \{ | \sum_{m=1}^{M} [\sum_{k=1+m}^{3N+m} \alpha_k I_k^{p*}(\theta_s,\phi_s)$$

$$+ \sum_{k=3N+1+m}^{6N+m} \alpha_k I_k^{p*}(\theta_s,\phi_s)] |^2 \qquad (5.1)$$

$$+ | \sum_{m=1}^{M} [\sum_{k=1+m}^{3N+m} \alpha_k I_k^{s*}(\theta_s,\phi_s)$$

$$+ \sum_{k=3N+1+m}^{6N+m} \alpha_k I_k^{s*}(\theta_s,\phi_s) |^2 \}$$

Eq. (5.1) could be expressed more compactly by not grouping the summations over k into subsums of 3N terms, but this grouping is necessary in (5.2) and in fact corresponds to the data storage procedure used in our computing code.

To determine the integrated or total scattering cross-section the integration over ϕ_s can be performed analytically leading to the result

$$\tilde{\sigma}_B(\theta_s) = \pi (4\pi k_0)^{-2} \sum_{m=1}^{M} [| \sum_{k=1+m}^{3N+m} \alpha_k I_k^{p*}(\theta_s,\pi/2m) |^2$$

$$+ | \sum_{k=1+m}^{3N+m} \alpha_k I_k^{s*}(\theta_s,0) |^2 + | \sum_{k=3N+1+m}^{6N+m} \alpha_k I_k^{p*}(\theta_s,0) |^2$$

$$+ | \sum_{k=3N+1+m}^{6N+m} \alpha_k I_k^{s*}(\theta_s,\pi/2m) |^2] . \qquad (5.2)$$

The integration over θ_s must be done numerically leading to the following results:

Total Scattering Cross-Section

$$\sigma_{TS} = \int_0^{\pi} \tilde{\sigma}_B(\theta_s) \sin\theta_s \, d\theta_s \qquad (5.3)$$

Absorption Cross-Section

$$\sigma_A = -I_m(n^2)|n^2-1|^{-2}k_0^{-2}\sum_{i=1}^{K}\sum_{j=1}^{K}\alpha_i\alpha_j{}^*W_{ij} \qquad (5.5)$$

Total or Extinction Cross-Section

$$\sigma_T = \sigma_{TS} + \sigma_A \qquad (5.6)$$

Assymmetry Factor

$$\sigma_{ASY} = \int_0^\pi \tilde{\sigma}_B(\theta_s)\sin\theta_s \, \cos(\theta_s-\theta_0)d\theta_s \qquad (5.7)$$

The forward scatter theorem* provides a relationship between σ_T and the component of the far-zone scattered electric field which is parallel to the incident electric vector (assuming plane incident polarization) and which is propagating directly forward; that is, in the same direction as the incident wave so that $\theta_s=\theta_0$, $\theta_s=\theta_0$. This relationship provides a check on σ_T as determined by (5.6) although one would expect its accuracy to be less for approximate numerical solutions such as ours. This is true partly because the theorem hangs the entire determination of σ_T on the value of the field in one direction; there is no smoothing of errors by integration as there is in (5.3) which provides one term in (5.6). A second reason is that the theorem is based on the interactions between excitations of the various elements of the scatterer. It will not apply for an approximate theory which does not take these into account sufficiently accurately. For example it does not hold for lowest order Rayleigh theory (Van de Hulst, 1957) and would not hold for our analysis if we had not adequately taken account of interelement interactions in the impedance evaluations. In any case we have programmed and evaluated the following

*Formula (110) Section 13.5 of Born and Wolf (1959 or 1975). We will apply the theorem for elliptical incident polarization and so use a slight generalization of the derivation and formula in Born and Wolf since they considered only plane incident polarization.

formula which is derivable directly from the forward scatter theorem. We use the notation of Section 4.

Extinction Cross-Section

$$\sigma_T = k_0^{-2} I_m \{p^* \sum_{k=1}^{3NM} \alpha_k I_k^{p*}(\theta_0, \phi_0) + q^* \sum_{k=1}^{3NM} \alpha_k I_k^{s*}(\theta_0, \phi_0)\} \qquad (5.8)$$

4. Computational Code and Results

A skeletal description of the FORTRAN programs for numerically evaluating the formulas detailed in Section 3 follows. All equation numbers refer to the numbering in that section.

Programs ZMAIN and WMAIN govern computation and storage of the symmetric complex matrices $\underline{Z}$ and $\underline{W}$ respectively. In each case the matrices are packed for storage into vectors using column major order using separate vectors corresponding to each of the 3N x 3N submatrices for each m value. The matrices were stored since the slowest and most expensive part of the program lies in computing the $\underline{Z}$ elements, yet they are needed for each computation involving the same disc dimensions relative to wavelength regardless of different incident wave amplitudes, directions and polarizations or different disc materials. The $\underline{W}$ matrix elements, although inexpensive to compute are similarly reusable.

Each of the submatrices is calculated by separate subroutines: ZTMO, ZTM1, ZEOM1, ZTM1 for Eqs. (2.24) - (2.27) corresponding to the different mode combinations for $\underline{Z}$ elements and WTMO, WTEO, WEOM1, WTM1 for Eqs. (3.6) - (3.9) for the $\underline{W}$ elements.

The excitations, Eqs. (4.5) are computed as needed for specified incident waves by program IMAIN using function subprograms for the sums

of Eq. (4.2). The excitation values are not stored since they are very inexpensive to compute.

Program AMAIN uses the stored $\underset{\sim}{Z}$ and $\underset{\sim}{W}$ elements plus the excitations computed by IMAIN to solve Eq. (1.1) for the coefficients α_k with the help of subfunctions CSPCO and CSPCL available on the Michigan Terminal System (MTS). CSPCO computes the condition number and a decomposition of matrix $\underline{z} = \underline{Z} - \underline{W} / (n^2 - 1)$ into the form $\underline{UDU}^*$ where $\underline{U}$ is a product of elementary unit lower triangular and permutation matrices and $\underline{D}$ is a block diagonal matrix with blocks of order 1 or 2. CSPSL then solves for the α_k by back substitution.

Finally, program XSECTS governs computation and printing of the various cross-sections, Eqs. (5.1) - (5.8). The cross sections, and all auxiliary functions are computed in function subroutines. The integrations involved are done by calling subroutine QCRP, an adaptive quadrature scheme available in the MTS system.

Apart from debugging the program we have had time and money on the grant to obtain only a few illustrative numerical results. Tables 1(a)-(c) list normalized* cross-sections for a disc of normalized dimensions a = 2.95, δ = 0.1 irradiated by plane polarized radiation of wavelength λ = 3.0 μm and composed of ice. This wavelength corresponds to the center of an infrared absorption band for ice and the refractive index is n = 1.130 - i0.2273. To exhibit how the <u>scattering</u> was influenced by the absorptivity we also list $\sigma_B(\theta_s, \phi_s)$ results for n = 1.130, $I_m n = 0$.

Results are presented for three incidence angles, θ_o=0° (broadside), θ_o=45° and θ_o = 90° (edge-on), each incident wave propagating in the x-z (ϕ=0°) plane with electric vector parallel to the y axis. For each incidence

---

*Length units are k_o^{-1}.

angle three scattering patterns are presented; i.e., $\sigma_B(\theta_s, \phi_s)$ as a function of θ_s for fixed values of ϕ_s; ϕ_s = 0°, 90° and 180°. When θ_o = 90° the forward scatter directions correspond to ϕ_s = 180° and the backscatter directions to ϕ_s=0°. We also list the values of σ_{TS} and σ_T; the latter computed both by Eq. (5.6) and Eq. (5.8), and the assymetry factors.

We note the agreement in the σ_T values obtained by integration and by the forward scatter theorem. In light of the discussion just prior to (5.8) it may therefore be inferred that the computed induced current is quite accurate. The listed data clearly show various flat disc scattering characteristics which are radically different from those of particle scattering. Thus for broadside incidence the scattering is symmetric in the forward and backward hemispheres corresponding to the 0° < θ_s < 90° and 90° < θ_s < 180° results while in the plane of the disc in the direction of $\overline{E}$ the scattering drops almost to zero. The resemblance to Rayleigh scattering from a sphere, simple dipole radiation is strong. On the other hand there is an appreciable forward to backward assymmetry for edge-on incidence; a forward bulge and a depression in the direct backscatter direction. There is also only a mild dip in the scattering pattern in the plane of the disc in the direction of the incident E vector; i.e., for θ_s = ϕ_s = 90°. Thus there is no vestige of the independence to particle orientation which is inherent for spherical scatterers.

The pattern for broadside incidence can be thought of as due to a superposition of parallel thin dipole currents in the $\hat{y}$ direction induced by the incoming electric field and all excited and radiating almost in phase because δ << 1. The effects of the loop currents generated by the incident magnetic field is negligible since oppositely

directed current elements on the top and bottom surfaces can be thought of as giving mutually cancelling radiations because they too are radiating in phase.

For edge-on incidence the pertinent phase differences for excitation and radiation are not small since the disc diameter is about a wavelength.   Hence the $\hat{y}$ directed dipoles due to incident $\underset{\sim}{E}$ are not excited in phase so that forward to backward symmetry should not be expected. Similarly the oppositely directed current elements in the current loops induced by the incident magnetic field need not produce mutually cancelling fields. In this way one can explain the "fill-in" of the pattern in the plane of the disc (relative to the almost zero result purely $\hat{y}$ directed current elements would yield) as being due to the circumferential current components.

Table 1. Normalized Cross Sections for disc, a=2.95, δ=0.1 with incident electric polarization parallel to flat disc surface

(a) Broadside direction of incidence, $\theta_0=0°$

BISTATIC CROSS SECTION $\sigma_B(\theta_s, \phi_s)$

θ_s degs.	n = 1.130 - i0.2273			n = 1.130	
	ϕ_s 0°	ϕ_s 90°	ϕ_s 180°	ϕ_s 0°	ϕ_s 90°
0	0.169E-01	0.169E-01	0.169E-01	0.453E-02	0.453E-02
10	0.159E-01	0.154E-01	0.159E-01	0.426E-02	0.411E-02
20	0.133E-01	0.115E-01	0.133E-01	0.357E-02	0.307E-02
30	0.998E-02	0.707E-02	0.998E-02	0.269E-02	0.189E-02
40	0.689E-02	0.363E-02	0.689E-02	0.187E-02	0.978E-03
50	0.451E-02	0.156E-02	0.451E-02	0.124E-02	0.423E-03
60	0.293E-02	0.561E-03	0.293E-02	0.816E-03	0.153E-03
70	0.201E-02	0.163E-03	0.201E-02	0.564E-03	0.477E-04
80	0.154E-02	0.295E-04	0.154E-02	0.437E-03	0.818E-05
90	0.140E-02	0.362E-14	0.140E-02	0.398E-03	0.102E-14
100	0.154E-02	0.163E-03	0.154E-02	0.437E-03	0.818E-05
110	0.201E-02	0.561E-03	0.201E-02	0.564E-03	0.447E-04
120	0.293E-02	0.156E-02	0.293E-02	0.816E-03	0.153E-03
130	0.451E-02	0.363E-02	0.451E-02	0.124E-02	0.423E-03
140	0.689E-02	0.707E-02	0.689E-02	0.187E-02	0.978E-03
150	0.998E-02	0.115E-01	0.998E-02	0.269E-02	0.190E-02
160	0.133E-01	0.154E-01	0.133E-01	0.357E-02	0.307E-02
170	0.159E-01	0.154E-01	0.159E-01	0.426E-02	0.411E-02
180	0.169E-01	0.169E-01	0.169E-01	0.453E-02	0.452E-02

	n = 1.130 - i0.2273		n = 1.130	
ABSORPTION CROSS SECTION	0.145E+01	1.61 DB	0.0	0.0
TOTAL SCATTERING CROSS SECTION	0.457E-01	-13.4 DB	0.124E-01	-19.1 DB
TOTAL CROSS SECTION EQ. (5.6)	0.149E+01	1.64 DB	0.124E-01	-19.1 DB
TOTAL CROSS SECTION EQ. (5.8)	0.151E+01	1.80 DB	0.183E-01	-17.4 DB
ASSYMMETRY FACTOR	0.743E-09		0.768E-09	

Table 1(b). 45° direction of incidence, θ_o = 45°

BISTATIC CROSS SECTION $\sigma_B(\theta_s, \phi_s)$

θ_s degs.	n = 1.130 - i0.2273			n = 1.130	
	ϕ_s 0°	ϕ_s 90°	180°	ϕ_s 0°	ϕ_s 90°
0	0.560E-02	0.560E-02	0.560E-02	0.153E-02	0.153E-02
10	0.745E-02	0.516E-02	0.384E-02	0.201E-02	0.140E-02
20	0.901E-02	0.411E-02	0.244E-02	0.241E-02	0.111E-02
30	0.996E-02	0.299E-02	0.148E-02	0.265E-02	0.785E-03
40	0.102E-01	0.216E-02	0.884E-03	0.272E-02	0.550E-03
50	0.991E-02	0.168E-02	0.546E-03	0.264E-02	0.417E-03
60	0.932E-02	0.143E-02	0.362E-03	0.249E-02	0.351E-03
70	0.872E-02	0.130E-02	0.266E-03	0.233E-02	0.317E-03
80	0.829E-02	0.123E-02	0.220E-03	0.222E-02	0.299E-03
90	0.814E-02	0.121E-02	0.206E-03	0.218E-02	0.293E-03
100	0.829E-02	0.123E-02	0.220E-03	0.222E-02	0.299E-03
110	0.872E-02	0.130E-02	0.266E-03	0.233E-02	0.317E-03
120	0.932E-02	0.143E-02	0.362E-03	0.249E-02	0.351E-03
130	0.991E-02	0.168E-02	0.546E-03	0.264E-02	0.417E-03
140	0.102E-01	0.216E-02	0.884E-03	0.272E-02	0.550E-03
150	0.996E-02	0.299E-02	0.148E-02	0.265E-02	0.785E-03
160	0.901E-02	0.411E-02	0.244E-02	0.241E-02	0.111E-02
170	0.745E-02	0.516E-02	0.384E-02	0.201E-02	0.140E-02
180	0.560E-02	0.560E-02	0.560E-02	0.153E-02	0.152E-02

ABSORPTION CROSS SECTION
0.114E+01   0.55 DB   0.0

TOTAL SCATTERING CROSS SECTION
0.330E-01   -14.8 DB   0.878E-02   -20.6 DB

TOTAL CROSS SECTION EQ. (5.6)
0.117E+01   0.67 DB   0.878E-02   -20.6 DB

TOTAL CROSS SECTION EQ. (5.8)
0.117E+01   0.67 DB   0.723E-02   -21.4 DB

ASSYMMETRY FACTOR
0.162E-01   0.428E-02

Table 1(c). Edge-on direction of incidence, $\theta_0 = 90°$

BISTATIC CROSS SECTION $\sigma_B(\theta_s, \phi_s)$

	$n = 1.130 - i0.2273$			$n = 1.130$	
θ_s degs.	ϕ_s 0°	ϕ_s 90°	180°	ϕ_s 0°	ϕ_s 90°
0	0.140E-02	0.140E-02	0.140E-02	0.398E-03	0.398E-03
10	0.252E-02	0.135E-02	0.729E-03	0.694E-03	0.380E-03
20	0.407E-02	0.128E-02	0.398E-03	0.110E-02	0.343E-03
30	0.583E-02	0.129E-02	0.258E-02	0.157E-02	0.316E-03
40	0.746E-02	0.126E-02	0.212E-03	0.200E-02	0.310E-03
50	0.870E-02	0.129E-02	0.207E-03	0.233E-02	0.313E-03
60	0.946E-02	0.129E-02	0.218E-03	0.253E002	0.312E-03
70	0.983E-02	0.126E-02	0.233E-03	0.263E-02	0.303E-03
80	0.996E-02	0.122E-02	0.242E-03	0.267E-02	0.293E-03
90	0.999E-02	0.121E-02	0.246E-03	0.268E-02	0.289E-03
100	0.996E-02	0.122E-02	0.242E-03	0.267E-02	0.293E-03
110	0.982E-02	0.126E-02	0.232E-02	0.263E-02	0.303E-03
120	0.946E-02	0.129E-02	0.218E-03	0.252E-02	0.312E-03
130	0.870E-02	0.129E-02	0.207E-03	0.233E-02	0.313E-03
140	0.746E-02	0.126E-02	0.211E-03	0.200E-02	0.310E-03
150	0.583E-02	0.124E-02	0.258E-03	0.157E-02	0.316E-03
160	0.407E-02	0.128E-02	0.398E-03	0.110E-02	0.343E-03
170	0.252E-02	0.135E-02	0.729E-03	0.694E-03	0.380E-03
180	0.140E-02	0.140E-02	0.140E-02	0.398E-03	0.398E-03

ABSORPTION CROSS SECTION	0.114E+01	0.55 DB		0.0	
TOTAL SCATTERING CROSS SECTION	0.231E-01	-16.4 DB		0.612E-02	-22.1 DB
TOTAL CROSS SECTION EQ. (5.6)	0.116E+01	0.65 DB		0.612E-02	-22.1 DB
TOTAL CROSS SECTION	0.116E+01	0.65 DB		0.516E-02	-22.9 DB
ASSYMMETRY FACTOR	0.182E-01			0.479E-02	

References

1. Auer, August H. Jr., and Donald L. Veal, (1970), "The Dimensions of Ice Crystals in Natural Clouds", J. Atmospheric Sciences, 27, pp. 919-926.

2. Born, Max and Emil Wolf, (1959), (1975), "Principles of Optics", Pergamon Press.

3. Chu, C-M., and Herschel Weil, (1976), "Integral Equation Method for Scattering and Absorption of Electromagnetic Radiation by Thin Lossy Dielectric Discs", J. Computational Physics, 22, pp. 111-124.

4. Van de Hulst, (1957), "Light Scattering by Small Particles", Wiley, p. 66.

5. Weil, Herschel and C-M. Chu, (1976), "Scattering and absorption of electromagnetic radiation by thin dielectric discs", Applied Optics, 15, pp. 1832-1836.

6. Zikmunda J. and Gabor Vali, (1972), "Fall Patterns and Fall Velocities of Rimed Ice Crystals", J. Atmospheric Sciences, 29, pp. 1334-1347.